Supplementary information

Avoiding Electrochemical Indentations: CNT-cocooned $LiCoO_2$ Electrode with Ultra-stable High-voltage Cycling

Zhi Zhu[a,b]*, Shuanglong Xu[a], Zhenjie Wang[a], Xiaohui Yan[a], Guiyin Xu[b], Yimeng Huang[c], Yuping Wu[a], Yin Zhang[b]* and Ju Li[b,c]*

[a] Confucius Energy Storage Lab, School of Energy and Environment & Z Energy-storage Center, Southeast University, Nanjing, Jiangsu, 211189, CN

[b] Department of Nuclear Science and Engineering, Massachusetts Institute of Technology, Cambridge, MA 02139, USA

[c] Department of Materials Science and Engineering, Massachusetts Institute of Technology, Cambridge, MA 02139, USA

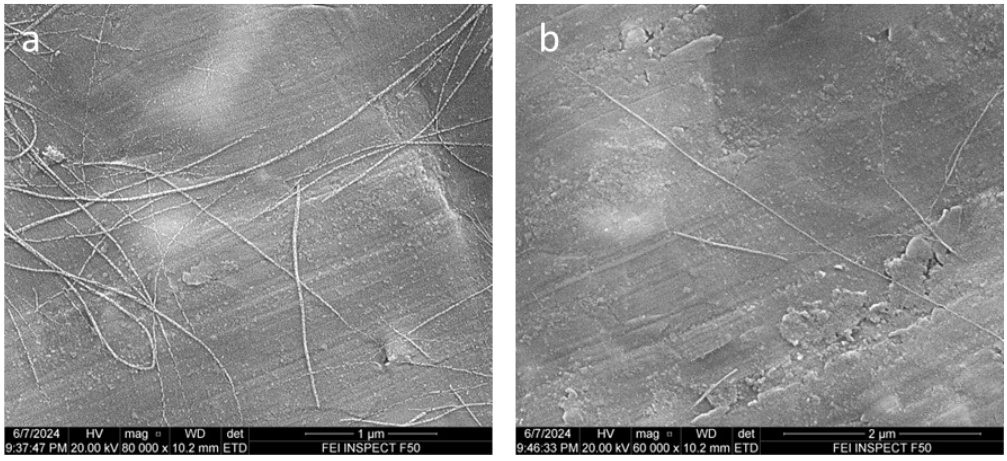

Supplementary Fig. 1 The morphology of the CNT used CNT-LCO

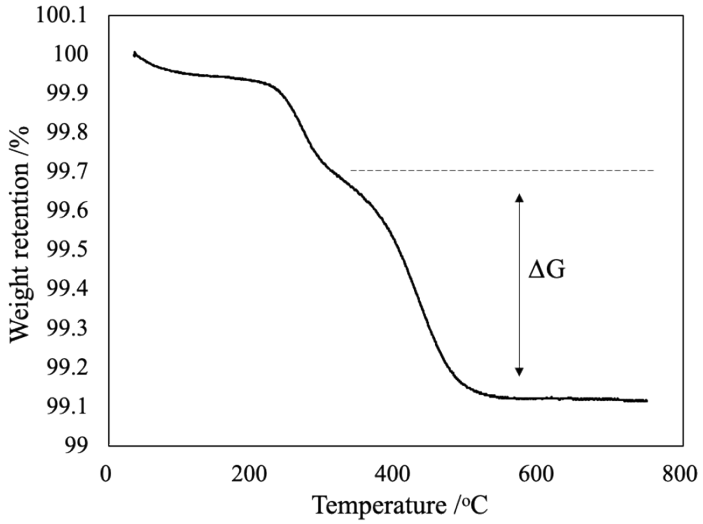

Supplementary Fig. 2 The TGA analysis of the CNT-LCO electrode in air, where the CNT decomposition occurred at above 300 °C and had a weight loss about 0.5%

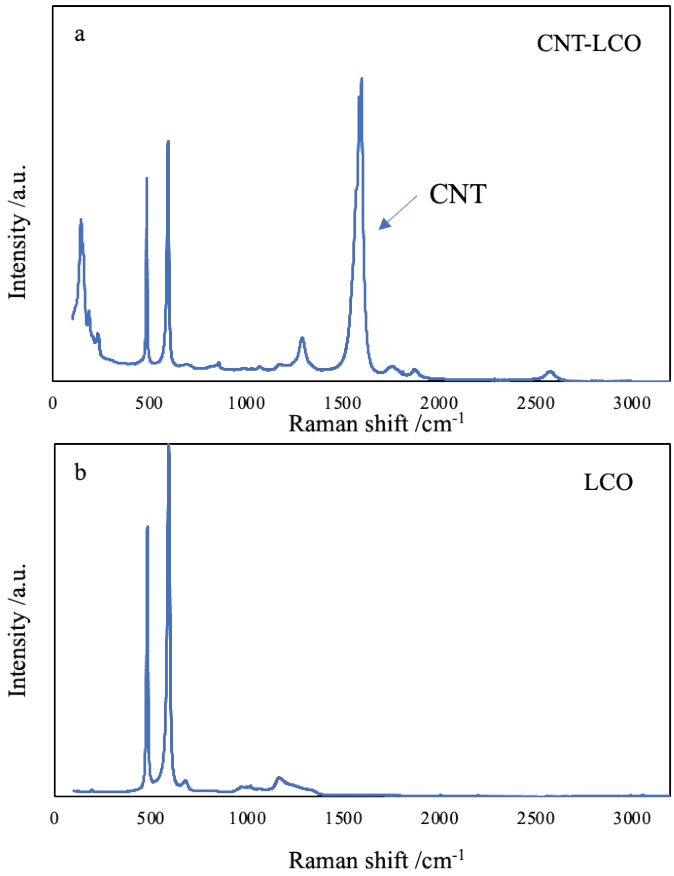

Supplementary Fig. 3 The Raman analysis of the CNT-LCO electrode and pure LCO particles

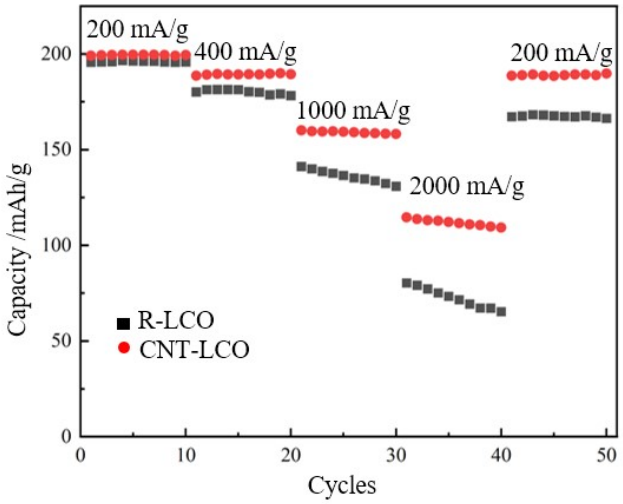

Supplementary Fig. 4 The cycling performance of R-LCO and CNT-LCO under different current density

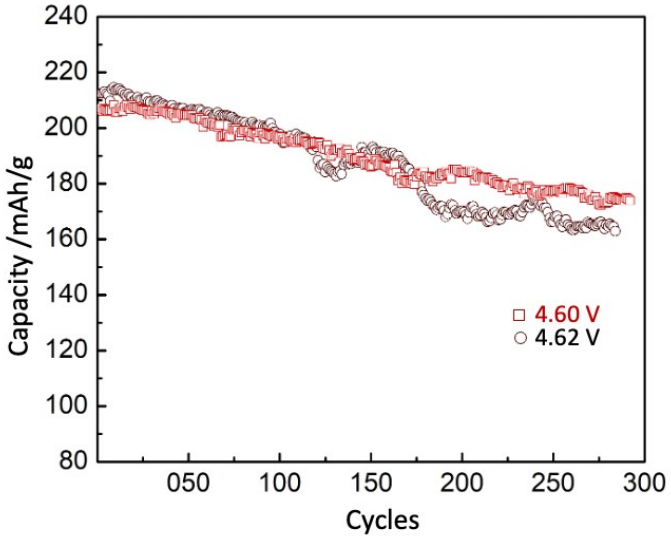

Supplementary Fig. 5 The cycling performances of CNT-LCO with the upper voltages of 4.60 V and 4.62 V.

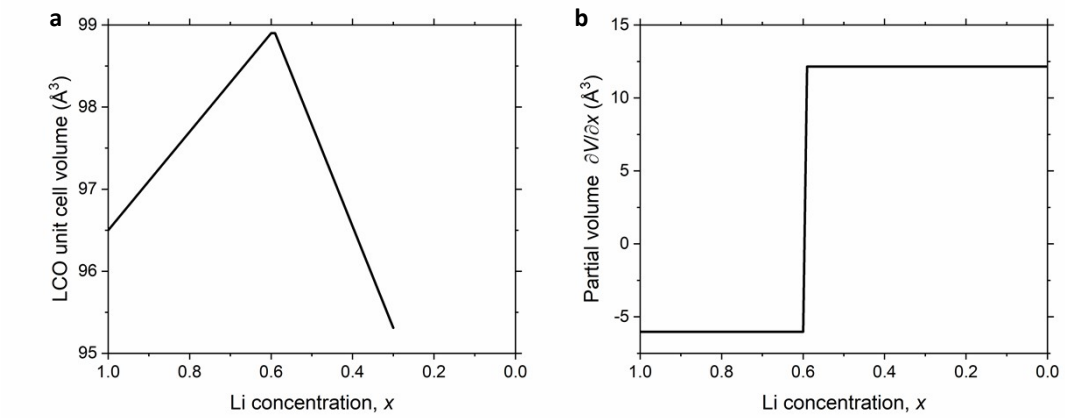

Supplementary Fig. 6 (a) The piecewise linear relationship between the LCO unit cell volume and Li concentration. (b) The partial volume of Li with respect to the Li concentration

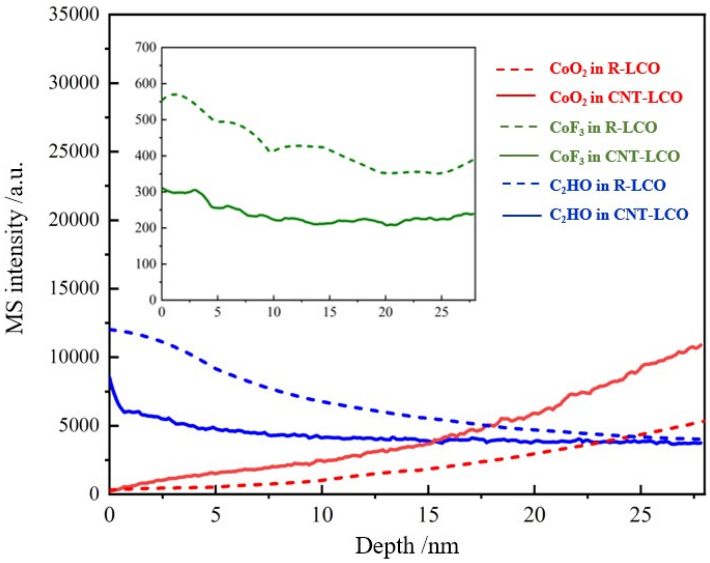

Supplementary Fig. 7 The depth profile of CoO_2, CoF_3 and C_2HO species at the surface of R-LCO and CNT-LCO after high voltage cycles

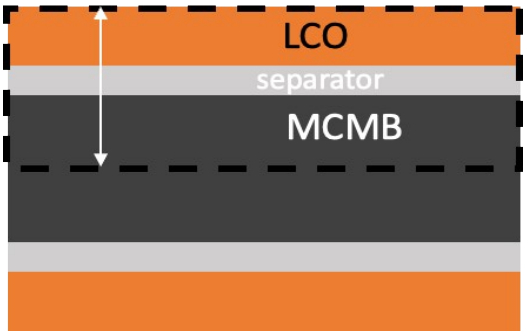

Supplementary Fig. 8 The new structures of the full-cells that designed for the free-standing electrodes.

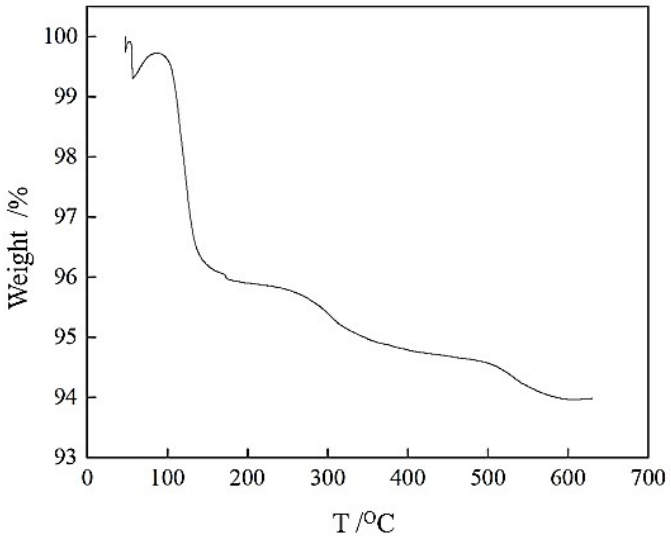

Supplementary Fig. 9 The TG analysis of the cycled CNT-LCO

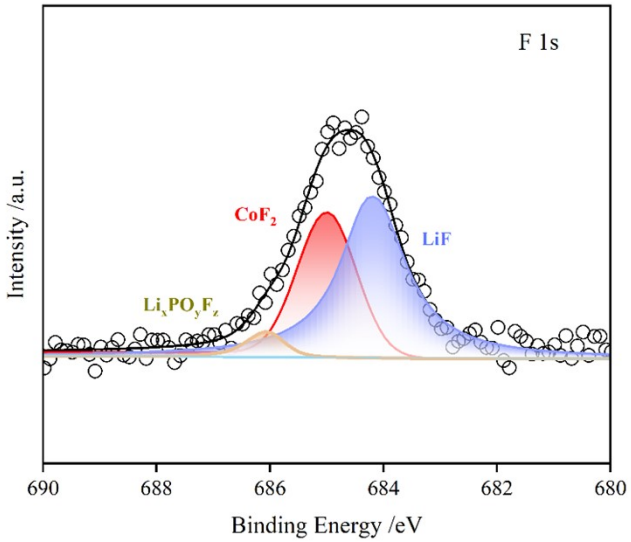

Supplementary Fig. 10 The XPS analysis of F on the surface of the regenerated LCO

Supplementary Table. 1 The details of CNT used for CNT-LCO

CNT specification	unit of measure	value
carbon content)	wt.%	99±1
CNT content)	wt.%	≥93
number of walls CNT	unit	1
outer mean diameter	nm	1.6±0.4
length of CNT	μm	>5
metal impurities	wt.%	<1

moisture	wt.%	<5

Supplementary Table. 2 The voltage changes in the GITT tests of R-LCO and CNT-LCO. Considering that $L \propto \frac{\eta 1}{\eta 2}$, the ratio of L in R-LCO to that in CNT-LCO can be estimated from the ratio of $\frac{\eta 1}{\eta 2}$ in the two materials.

	10th cycle				300th cycle			
	IR_Ω	η_1	η_2	η_1/η_2	IR_Ω	η_1	η_2	η_1/η_2
R-LCO	0.0506 V	0.0532 V	0.0294 V	1.81	0.2173 V	0.08 V	0.0127 V	6.30
CNT-LCO	0.0487 V	0.0435 V	0.0271 V	1.60	0.0554 V	0.0534 V	0.0268 V	1.99

Supplementary Table. 3 The loading of free-standing cathode and anode materials for pouch full-cells

	mAh/cm²	mg/cm²	g/cm³	mAh/g	CNT%
CNT-LCO	6	30.8	4.3	195	0.5
CNT-MCMB	6.5	18.6	1.7	350	1

Supplementary Discussion

Based on the structure of pouch full cell and loadings of cathode and anodes shown in Fig. 8 and Table. 3, the energy density can be evaluated with the following methods.

(1) For the volumetric energy density (*E*v),

$d_{cathode}$ = 71.6 um

d_{anode} = 109.4 um

d_{sep}= 12 um

$d = d_{cathode} + d_{sep} + d_{anode}$ = 193 um

*E*v = 1212.5 Wh/L

(2) For the weight energy density (*E*w),

$L_{separator}$ = 0.8 mg/cm²

$L_{electrolyte}$ = 2 g/Ah (12 mg/cm²)

Ew = 376.2 Wh/kg

If includes the weight of tabs used in the full-cell, where 20 layers of cathode/anode were assembled in each unit cell, the energy density can be estimated as

$m_{\text{Al tab}}$ = 32 mg,

$m_{\text{Ni tab}}$ = 94 mg,

Ew = 341 Wh/kg